An experimental study of the influence of graphite on the electrical conductivity of olivine aggregates

Duojun Wang,[1,2] Shun-ichiro Karato,[2] and Zhenting Jiang[2]

Received 28 February 2013; revised 3 April 2013; accepted 12 April 2013; published 31 May 2013.

[1] Presence of graphite is one of the mechanisms to explain enhanced electrical conductivity. Because the conductivity of graphite is highly anisotropic and the connectivity of graphite depends strongly on the geometry of the crystals, the key issue is the geometry of graphite in a rock including their crystallographic orientation and the shape of graphite crystals. We explored the role of graphite on electrical conductivity in olivine-rich aggregates. To obtain well-defined results, we conducted an experimental study at high pressure and temperature conditions. Olivine aggregates containing diamonds were annealed to transform diamond to graphite with nearly equilibrium morphology. Graphite formed by the transformation from diamond has thin disk-shape morphology, the plane being the highly conductive (0001) plane. When the concentration of graphite exceeds the percolation threshold (~ 1 wt%), electrical conductivity is significantly enhanced. Some of the observed high conductivity regions may represent regions of high concentration of graphite. **Citation:** Wang, D., S.-i. Karato, and Z. Jiang (2013), An experimental study of the influence of graphite on the electrical conductivity of olivine aggregates, *Geophys. Res. Lett.*, *40*, 2028–2032, doi:10.1002/grl.50471.

1. Introduction

[2] The regions of high electrical conductivity in Earth have attracted much attention because they may correspond to regions of anomalous compositions including the presence of fluids or melts [*Shankland and Ander*, 1983; *Gaillard et al*., 2008], high hydrogen content [*Karato*, 1990; *Wang et al*., 2006; 2008; *Yoshino et al*., 2006; 2009; *Poe et al*., 2010], and high carbon content as graphite [*Duba and Shankland*, 1982; *Glover and Vine*, 1992]. Carbon and hydrogen are the two important volatile elements in Earth's interior. They occur roughly the same amount in the mantle [*Wood et al*., 1996; *Dasgupta and Hirschmann*, 2010], and both elements promote melting [*Kushiro*, 2001; *Gaillard et al*., 2008; *Green et al*., 2010; *Dasgupta and Hirschmann*, 2006; 2007] and control the nature of Earth's atmosphere [*Kasting and Catling*, 2003], and therefore the evolution of Earth including its surface conditions such as the habitability [*Kasting and Catling*, 2003]. A large number of studies have been performed to infer hydrogen distribution in Earth's interior [*Karato*, 2003; *Dixon et al*., 2002; *Karato*, 2011]. In addition to direct, petrological (or geochemical) approach [*Dixon et al*., 2002], remote sensing of hydrogen is possible because of the sensitivity of electrical conductivity to hydrogen content [*Wang et al*., 2006; *Yoshino et al*., 2009; *Karato*, 2011; *Yang* et al., 2012].

[3] In contrast, remote sensing of carbon is more challenging because the solubility of carbon in many minerals is low [*Shcheka et al*., 2006], and the influence of carbon on physical properties is in most cases minor. The low solubility of carbon in mantle minerals means that carbon occurs in isolated carbon-bearing phases in most cases. The stable carbon-bearing species in the mantle depends on the pressure, temperature, and oxygen fugacity [*Frost and Wood*, 1997; *Kennedy and Kennedy*, 1976]. At relatively low pressure and low oxygen fugacity conditions, carbon occurs as graphite and because graphite has high and anisotropic electrical conductivity (conductivity in the (0001) plane is higher than conductivity in the direction normal to this plane by a factor of ~10^4) [*Dutta*, 1953], the presence of graphite could be detectable through electrical conductivity if there is enough graphite with appropriate crystallographic orientations.

[4] However, previous studies on the influence of graphite on electrical conductivity were limited for several reasons. First, there was little direct experimental study where the electrical conductivity of graphite-bearing rock was measured under the upper mantle conditions. Most of previous studies were conducted under the crustal conditions [*Glover and Vine*, 1992; *Duba et al*., 1988], and the geometry of graphite is likely out of equilibrium. *Watson et al*. [2010] conducted an experimental study under the upper mantle conditions, but they did not observe appreciable effects of graphite presumably because of a small amount (~0.1 wt%) of graphite they added. Y*oshino and Noritake* [2011] conducted an experimental study on the quartz-graphite system where higher temperature (to 1200 K) was used to study the morphology of graphite, but the relevance of their study to the upper mantle conductivity is questionable because the morphology of a secondary phase depends on the interfacial energy that depends on the host mineral. Second, in many studies, the presence of amorphous graphite at grain boundaries was considered [*Duba and Shankland*, 1982; *Glover and Vine*, 1992], but amorphous graphite unlikely occurs under the (deep) upper mantle conditions. Electrical conductivity of single crystal of graphite is highly anisotropic [*Dutta*, 1953] and therefore the

[1]Key Laboratory of Computational Geodynamics, University of Chinese Academy of Sciences, Beijing, China.
[2]Yale University, Department of Geology and Geophysics, New Haven, USA.

Corresponding author: Duojun Wang, Key Laboratory of Computational Geodynamics, University of Chinese Academy of Sciences, Beijing, 100049, China. (duojunwang@hotmail.com)

0094-8276/13/10.1002/grl.50471

Table 1. Conditions of Annealing Experiments and the Observed Volume Fraction of Graphite, and its Morphology (c and w) and the Calculated Parameter p ($= \frac{\pi}{4}\phi\frac{c}{w}$)

Run	P (GPa)	T (K)	Capsule	Duration (hrs)	Products	φ	c (μ m)	w (μ m)	p
K1221	4	1673	Mo	11.5	Ol + G + D	0.04(1)	8(2)	0.55(15)	0.46(14)
K1242	4	1673	Re	10.0	Ol + M + D				
K1245	3	1673	Mo	20.0	Ol + G	0.07(1)	10(2)	0.85(15)	0.65(15)

Note: Ol, olivine; G, graphite; D, diamond; M, magnesite. Numbers in parentheses are the errors in the last digit (one standard deviation)

electrical conductivity of a rock containing graphite with equilibrium morphology needs to be studied to understand how graphite may enhance electrical conductivity.

2. Experimental Procedure

[5] We prepared a mixture (~10–15 μm) of olivine and ~5% wt diamond (+ ~1% wt orthopyroxene) and annealed them under the controlled oxygen fugacity at high pressure and temperature. The powdered staring materials were well mixed and loaded into a molybdenum or rhenium foil capsule which was used to buffer the oxygen fugacity. The annealing experiments were performed at T = 1673 K and P = 3, 4 GPa in a 1000-tonne multianvil apparatus (Table 1). The run duration varied from ~10 to ~20 h. In one set of experiment (annealing at low f_{O2}), the conditions were chosen where diamond transformed to graphite, and in another set of experiments (annealing at high f_{O2}), diamond transformed to magnesite (Figure 1). The volume fraction and morphology of graphite (and magnesite) were studied using scanning electron microscopy (SEM). Both energy-dispersive x-ray analysis and electron back-scatter diffraction were used to study the samples. In a sample annealed at high f_{O2}, diamond nearly completely disappeared and some magnesites are observed at grain boundaries as expected from the stability field of diamond [*Frost and Wood*, 1997]. In samples annealed at low f_{O2}, most of diamond transformed to graphite. In one sample (annealed for 11.5 h), the transformation was ~50 % whereas in another sample (annealed for 20 h), the transformation was nearly complete. In both cases, the graphite formed from the transformation of diamond occurred at grain boundaries and has well-defined plate-like morphology (Figure 2), the (0001) plane being the plane.

[6] Electrical conductivity of annealed samples (a disk-shape with 1.6 mm in the diameter and 0.4–0.7 mm in the thickness) was measured using the impedance spectroscopy at condition of T = 1173–1673 K and P = 4 GPa (Table 2). The procedure of conductivity measurements is the same

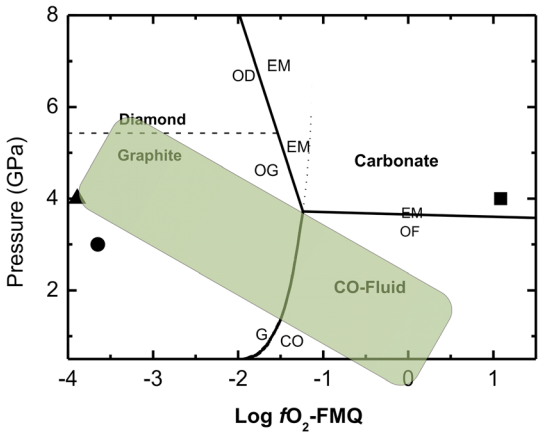

Figure 1. Experimental conditions (+ diamond-graphite stability field). The solid triangle denotes the experimental condition performed at 4.0 GPa and 1673 K buffered by Mo-MoO_2 for 11.5 h; the solid circle denotes the experimental conditions performed at 3.0 GPa and 1673 K buffered by Mo-MoO_2 for 20 h; the solid square denotes the experimental condition performed at 4 GPa and 1673 K buffered by the Re-ReO_2 for ~10 h. The carbon species stability fields were from *Frost and Wood* [1997]. G, graphite; D, diamond; E, enstatite; M, magnesite; F, Forsterite; O, oxygen; F, forsterite. A shaded region corresponds to conditions of the continental upper mantle inferred from xenoliths [*Frost and McCammon*, 2008].

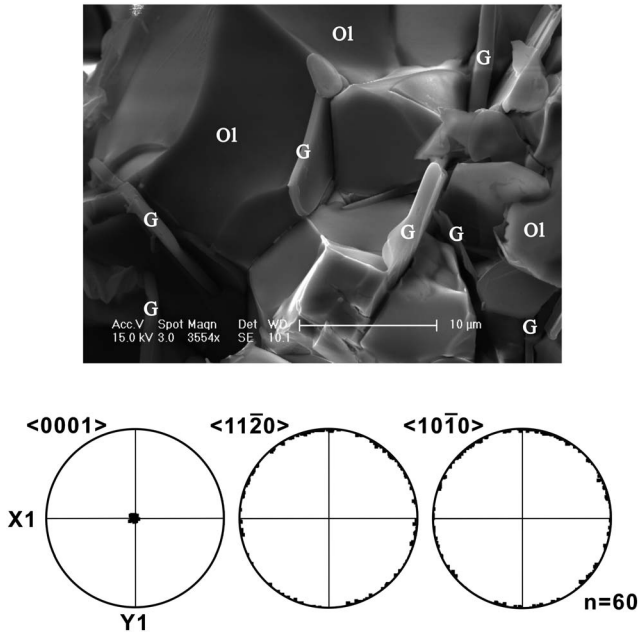

Figure 2. (a) A scanning electron microscope (SEM) microphotograph, (b) the orientations of graphite. (a) A scanning electron microscopy (SEM) image of a sample (K1221). The diamond transformed to graphite and graphite is present as disks in the olivine grain boundary. G indicates graphite; Ol is olivine. (b) A pole figure showing crystallographic orientations of 60 graphite crystals. Single crystals of disk-shaped graphite are collected from the sample, and their orientations are determined by electron back-scattered diffraction. The results show that the disk plane corresponds to the (0001) plane.

Table 2. The Experimental Conditions for Conductivity Measurements, and the Results of the Least-Square Fit Using the Formula $\sigma = A \cdot \exp(-\frac{H*}{RT})$

Run	P (GPa)	T (K)	Log_{10} A (S/m)	H* (kJ/mol)
K1231	4	873–1773 K	−1.10 (9)	16 (2)
K1251	4	873–1773 K	−0.02 (6)	82 (2)
K1253	4	873–1773 K	1.96 (2)	4 (1)

Note: K1251 denotes results of the sample (K1242) annealed for 10 h at high f_{O2}; K1231 and K1253 indicate the results of samples annealed at low f_{O2} at 11.5 h (K1221) and 20 h (K1245), respectively.

P: pressure, T: temperature.

Numbers in parentheses are the errors in the last digit (one standard deviation)

as before [e.g., *Wang et al.*, 2006]. The samples were then loaded between two Mo or Re electrodes that are insulated by the alumina rings. To minimize the noise coming from the heater, we used a shield. The shield, typically the same metal as that of the electrode, is located between the sample and MgO tube. The oxygen fugacity was buffered by the metal shield and electrodes. Complex impedance measurements were conducted using the Solartron 1260 frequency response analyzer operated at 0.1–1 V over the frequency range 1.0 Hz–1.0 MHz.

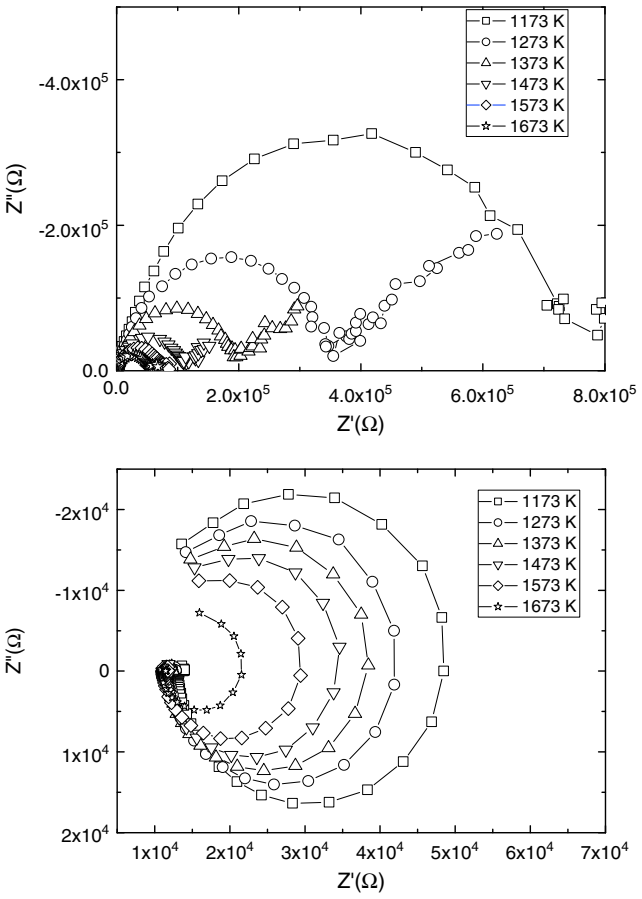

Figure 3. Impedance spectra of impedance spectra of magnesite-bearing sample (top) and graphite-bearing sample (bottom) at different temperatures.

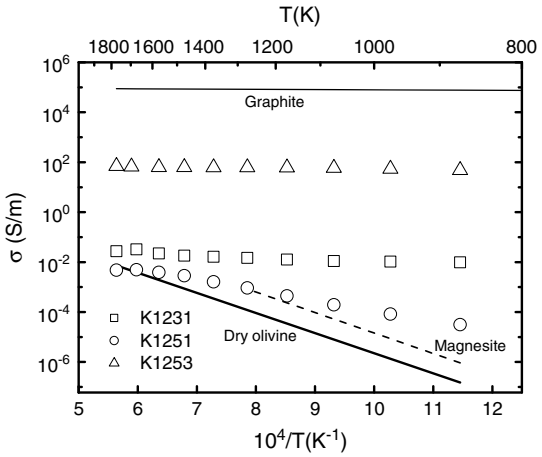

Figure 4. The electrical conductivity versus 1/T relationship (T: temperature). The solid thin line indicates electrical conductivity of graphite [*Duba and Shankland*, 1982]. The solid thick line denotes the dry olivine [*Constable*, 2006]. Dashed line is the electrical conductivity of magnesite ($MgCO_3$) [*Mibe and Ono*, 2011]. Open circles (K1251) denotes results of the sample annealed for 10 h at high f_{O2} (sample K1242); open squares (K1231) and triangles (K1253) indicate the results of samples annealed at low f_{O2} at 11.5 h and 20 h (samples K1221 and K1245), respectively. The error bars for electrical conductivity are smaller than the symbols.

3. Results and Discussions

[7] Figure 3 shows the representative impedance spectra of magnesite-bearing sample (a) and graphite-bearing sample (b) in the form of complex plane plots (real part (Z') versus imaginary part (Z'') of the impedance. In the magnesites-bearing sample, at given temperature, a

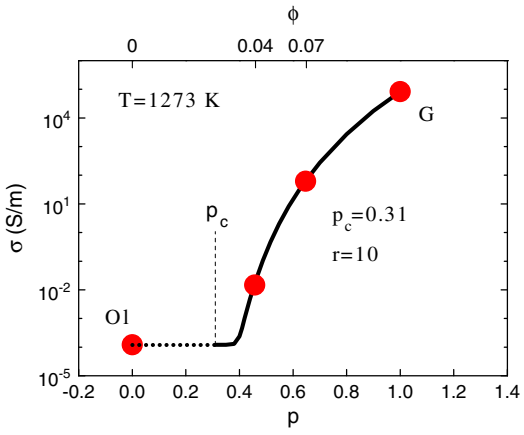

Figure 5. Electrical conductivity versus p. The electrical conductivity of olivine-bearing graphite (σ) was calculated as a function of a parameter p ($= \frac{\pi}{4}\varphi_w^c$) at 1273 K according to the Equations 2. A black line and solid circles show the observed conductivity values corresponding to given p. The parameter p is determined from the microstructural measurements. Our experimental data fit to equation (2) for p_c 0.3, $r = 10$. When $p < p_c$, the electrical conductivity of mixture is equal to that of olivine in the percolation model.

complete arc due to grain interior conduction and an incomplete arc (or tail) corresponding to grain boundary conduction are observed. The impedance spectra of graphite-bearing sample show the negative Z'' at high frequency and the positive Z'' indicative of the presence of inductive component at low frequency. The inductive component is often seen when chemical reactions occur (e.g., [*Macdonald*, 1978; *Bai and Conway*, 1991]). In both cases, DC component of conductivity can be determined from the first half-circle using an appropriate model.

[8] The results of electrical conductivity measurements are summarized in Figure 4 where the electrical conductivity of graphite containing samples is compared with that of pure olivine (+ opx) and a sample with magnesite. The uncertainty associated with these conductivity measurements is smaller than the symbol size. The FTIR measurements show that all the samples are for nearly dry (less than ~10 ppm wt). Samples containing magnesite or diamond show conductivity slightly higher than that of olivine, whereas samples containing graphite show much higher conductivity. Conductivity of graphite-bearing samples is high and depends only weakly on temperature. This suggests that the conductivity in these samples is controlled largely by graphite.

[9] The activation enthalpies (Table 2) were calculated by fitting the electrical conductivities according to the following equation:

$$\sigma = \mathrm{A}\exp\left(-\frac{H^*}{RT}\right) \tag{1}$$

where A is the pre-exponential factor, H* is the activation enthalpy, and R is the gas constant.

[10] In order for graphite to contribute to conductivity of aggregate, graphite grains need to be connected and the electric current dominantly flow in the (0001) plane. As shown in Figure 2, graphite grains are planar and the plane is (0001) in which the conductivity is highest [*Dutta*, 1953]. Therefore, if graphite grains are connected at edges, they will serve high conductivity path. The electrical conductivity of olivine and graphite mixture is dominated by olivine at a small volume fraction of graphite, but because graphite has much higher conductivity than olivine, the conductivity of an aggregate increases substantially once graphite grains are interconnected. Such a behavior can be described by the theory of percolation [*Gueguen and Dienes*, 1989]. The contribution from the high conductivity inclusion is negligible below the percolation threshold, but increases above the threshold following the relation,

$$\begin{aligned} \sigma &= (\sigma_0 - \sigma_m)\left(\frac{p - p_c}{1 - p_c}\right)^r + \sigma_m \quad \text{for} p \geq p_c \\ \sigma &= \sigma_m \qquad\qquad\qquad\qquad\quad \text{for} p < p_c \end{aligned} \tag{2}$$

where σ is the conductivity of the aggregate, σ_0 is the conductivity of a high conductivity inclusions (conductivity of graphite in the (0001) plane), σ_m is the electrical conductivity of the matrix (olivine), r is a nondimensional parameter, $p = \frac{\pi}{4}\varphi\frac{c}{w}$ (c: diameter of a graphite disk, w: thickness of the graphite disk), φ is the volume fraction of the high conductivity inclusions (graphite), p_c is the threshold value of p (percolation threshold) that depends on the geometry of conductor (graphite) [*Stauffer and Aharony*, 1994]. We determined the parameter p from the microstructural measurements (Table 1). We plotted the measured values of conductivity as a function of p (Figure 5). Fitting the experimental data to equation (2), we found that $r \sim 10$ and $p_c \approx 0.3$.

[11] Efficient enhancement of conductivity by the presence of graphite is largely due to the planar morphology ($\frac{c}{w} >> 1$) controlled by the anisotropy of the surface energy of graphite. The observed $\frac{c}{w} = 10$–20 is roughly consistent with the known anisotropy of surface energy of graphite that predicts $\frac{c}{w} = \frac{1}{2}\frac{\gamma_a}{\gamma_c}$ ($\frac{\gamma_a}{\gamma_c} \approx 50$ [*Abrahamson*, 1973; *Zaidi et al.*,1995], a small deviation from the simple model may be caused by the strain energy or by the influence of some impurities, γ_c is the surface (interface) energy of disk plane ((0001) plane), and γ_a the surface (interface) energy of a plane normal to the disk plane). In Earth's mantle, the morphology of graphite is likely near equilibrium, and in such a case, we may use $\frac{c}{w} = \frac{1}{2}\frac{\gamma_a}{\gamma_c}$ to estimate the percolation threshold to obtain $\varphi_c = \frac{8}{3\pi}\frac{\gamma_c}{\gamma_a} \approx 0.017$ volume fraction (~1 wt%).

[12] A majority of the geophysical observations of electrical conductivity in the upper mantle may be attributed to the conduction in an olivine + orthopyroxene mixture with the help of hydrogen [*Wang et al.*, 2006; *Karato*, 2011; *Dai and Karato*, 2009]. However, high conductivity regions in some of the continental upper mantle are difficult to explain by this mechanism because a majority of the continental lithosphere is depleted with water and relatively low temperatures [*Carlson et al.*, 2005] and temperatures in the relatively shallow part (~100 km or shallower) is not high (<1300 K). *Jones et al.* [2003] suggested that high conductivity regions (~0.1 S/m) at around the depth of ~100–120 km in the Western Canadian Shield may be produced by carbon, either as graphite or as carbon on grain boundary films. High conductivity (~0.1 S/m) at this depth (temperature ~ 1000–1300 K) is difficult to be attributed to the presence of hydrogen because more than ~0.1 wt% of water would be required [*Wang et al.*, 2006] exceeding the solubility limit of water in olivine. Using our results, we suggest that such high conductivity may be attributed to a large concentration of graphite (~1 wt%).

4. Conclusions

[13] The ability for graphite to enhance electrical conductivity depends on its volume fraction and geometry. A previous study [*Mathez*, 1987] suggested that only ~ 0.01 wt% carbon in mantle-derived rock is needed to create a good conductor (~0.1 S/m). However, their argument was based on the assumption that all grain boundaries are covered by amorphous graphite. *Watson et al.* [2010] showed that even up to 0.1 wt% carbon did not enhance the bulk conductivity of an olivine aggregate. Their observations are consistent with ours, but detailed interpretation cannot be made because they did not study the morphology of graphite.

[14] The critical fraction of graphite is different if graphite morphology is controlled by the surface energy. We report that graphite in olivine-rich matrix assumes highly anisotropic near equilibrium morphology under the upper mantle conditions. Such morphology promotes mutual connection of graphite grains along the orientations with high electrical conductivity (the (0001) plane). In such a case, ~1 wt% of

graphite will be needed to enhance electrical conductivity in some regions.

[15] The amount of carbon in Earth's mantle is highly uncertain. The published results range from ~0.001 wt% to ~1 wt% suggesting high regional variation in carbon content including both lateral and radial variation [e.g., *Dasgupta and Hirschmann*, 2010; *Deines*, 2002; *Wood et al*.,1996]. Typical oxygen fugacity in the upper mantle is about 1 to 3 log unit less than the oxygen fugacity corresponding to the FMQ buffer [*Frost and Mccammon*, 2008; *Frost and Wood*, 1997] (see Figure 1). This corresponds roughly to the limit of the stability field of graphite [*Frost and Wood*, 1997]. Therefore, we conclude that high conductivity regions at ~100–150 km depth might correspond to regions of high carbon content with typical or somewhat lower than typical oxygen fugacity, e.g., upper mantle above some subduction zones with a large amount of subducted sediments.

[16] **Acknowledgments.** We are grateful to Z. Du, G. Amulele, K. Otsuka, R. Farla, and Y.Guo for technical support. R. Dasgupta provided a discussion on the carbon content in the mantle. We thank three anonymous reviewers for their useful comments. This study was supported by the NSF of USA (EAR-0911465) and by the National Science Foundation of China (NSFC, Nos.40774036 and 41074063).

References

Abrahamson, J. (1973), The surface energies of graphite, *Crbon*, *11*, 337–362.

Bai, L., and B. E. Conway (1991), AC impedance of faradaic reactions involving electrosorbed intermediates: examination of conditions leading to pseudoinductive behavior represented in three dimensional impedance spectroscopy diagrams, *J. Electrochem. Soc.*, *138*, 2897–2907.

Carlson, R. W., D. G. Pearson, and D. E. James (2005), Physical, chemical, and chronological characteristics of continental mantle, *Rev. Geophys.*, *43*, doi:10.1029/2004RG000156.

Constable, S. (2006), SEO3: A new model of olivine electrical conductivity, *Geophys. J. Inter.*, *166*, 435–437.

Dai, L., and S. Karato (2009), Electrical conductivity of orthopyroxene: Implications for the water content of the asthenosphere, *Proc. Japan Acad.*, *85*, 466–475.

Dasgupta, R., and M. M. Hirschmann (2006), Melting in the Earth's deep mantle caused by carbon dioxide, *Nature*, *440*, 659–662.

Dasgupta, R., and M. M. Hirschmann (2007), Effect of variable carbonate concentration on the solidus of mantle peridotite, *Am. Mineral.*, *92*, 370–379.

Dasgupta, R., and M. M. Hirschmann (2010), The deep carbon cycle and melting in Earth's interior, *Earth Plane Sci. Lett.*, *298*, 1–13.

Deines, P. (2002), The carbon isotope geochemistry of mantle xenoliths, *Earth Sci. Rev.*, *58*, 247–278.

Dixon, J. E., L. Leist, J. Langmuir, and J. G. Schiling (2002), Recycled dehydrated lithosphere observed in plume-influenced mid-ocean-ridge basalt, *Nature*, *420*, 385–389.

Duba, A., and T. J. Shankland (1982), Free carbon and electrical conductivity in the Earth's mantle, *Geophy. Res. Lett.*, *9*, 1271–1274.

Duba, A., E. Huenges, G. Nover, G. Will, and H. Jödicke (1988), Impedance of black shale from Münsterland 1 borehole an anomalously good conductor?, *Geophys. J.*, *94*, 413–419.

Dutta, A. K. (1953), Electrical conductivity of single crystals of graphite, *Phys. Rev.*, *90*, 187–192.

Frost, D. J., and C. McCammon (2008), The redox state of Earth's mantle, *Ann. Rev. Earth Plane. Sci.*, *36*, 389–420.

Frost, D. J., and B. J. Wood (1997), Experimental measurements of the fugacity of CO_2 and graphite/diamond stability from 35 to 77 kbar at 925 to 1650 °C, *Geochim. Cosmochim. Acta*, *61*, 1565–1574.

Gaillard, F., M. Malki, G. Iacono-Maziano, M. Pichavant, and B. Scaillet (2008), Small Amount of carbonatite melts explains high electrical conductivity in the asthenosphere, *Science*, *322*, 1363–1365.

Glover, P. W. J., and F. J. Vine (1992), Elecrtical conductivity of carbon bearing granulite at raised temperatures and pressures, *Nature*, *360*, 723–726.

Green, D. H., W. O. Hibberson, I. Kovács, and A. Rosenthal (2010), Water and its influence on the lithosphere-asthenosphere boundary, *Nature*, *467*, 448–452.

Gueguen, Y., and J. Dienes (1989), Transport properties of rocks from statistics and percolation, *Mathe. Geology*, *21*, 1–13.

Jones, A. J., P. Lezaeta, I. J. Ferguson, A. J. Chave, R. L. Evans, X. Garcia, and J. Spratt (2003), The electrical structure of the Slave craton, *Lithos*, *71*, 505–527.

Karato, S. (1990), The role of hydrogen in the electrical conductivity of the upper mantle, *Nature*, *347*, 272–273.

Karato, S. (2003), Mapping water content in the upper mantle, in *Inside the Subduction Factory*, edited by J. Eiler, pp. 135–152, AGU monograph, Washington, D.C., *138*.

Karato, S. (2011), Water distribution across the mantle transition zone and its implications for global material circulation, *Earth Plane Sci. Lett.*, *301*, 413–423.

Kasting, J. F., and D. Catling (2003), Evolution of a habitable planet, *Ann. Rev. Astron. Astrophys.*, *41*, 429–463.

Kennedy, C. S., and G. C. Kennedy (1976), The equilibrium boundary between graphite and diamond, *J. Geophys. Res.*, *81*, 2467–2470.

Kushiro, I. (2001), Partial melting experiments on peridotite and origin of mid-ocean ridge basalt, *Ann. Rev. Earth Plan. Sci.*, *29*, 71–107.

Macdonald, D. (1978), A method for estimating impedance parameters for electrochemical systems for electrochemical systems that exhibit pseudoinductance, *J. Electrochem. Soc.Solid state Sci. Technol.*, *125*, 2062–2064.

Mathez, E. A. (1987), Carbonaceous matter in mantle xenoliths: Composition and relevance to the isotopes, *Geochim. Cosmochim. Acta*, *51*, 2339–2347.

Mibe, K., and S. Ono (2011), Electrical conductivityof $MgCO_3$ at high pressures and high temperatures, *Physica B*, *406*, 2018–2020.

Poe, B. T., C. Romano, F. Nestola, and J. R. Smyth (2010), Electrical conductivity anisotropy of dry and hydrous olivine at 8 GPa, *Phys. Earth Planet. Inter.*, *181*, 103–111, doi:10.1016/j.pepi.2010.05.003.

Shankland, T. J., and M. E. Ander (1983), Electrical conductivity, temperatures, and fluids in the lower crust, *J. Geophys. Res.*, *88*, 9475–9484.

Shcheka, S. S., M. Wiedenbeck, D. J. Frost, and H. Keppler (2006), Carbon solubility in mantle minerals, *Earth Plane. Sci. Lett.*, *245*, 730–742.

Stauffer, D., and A. Aharony (1994), *Introduction to Percolation Theory*, Taylor and Francis, London.

Wang, D., M. Mookherjee, Y. Xu, and S. Karato (2006), The effect of water on the electrical conductivity in olivine, *Nature*, *443*, 977–980.

Wang, D., H. Li, L. Yi, and B. Shi (2008), The electrical conductivity of upper mantle rocks: implication of water content in the upper mantle, *Phys.Chem.Minerals*, *35*, 157–162.

Watson, H. C., J. J. Roberts, and J. A. Tyburczy (2010), Effect of conductivity impurities on electrical conductivity in polycrystalline olivine, *Geophys. Res. Lett.*, *37*, L02302, doi:10.1029/2009GL041566.

Wood, B. J., A. R. Pawley, and D. R. Frost (1996), Water and carbon in the Earth's mantle, *Philoso. Trans. Royal Soc. London*, *354*, 1495–1511.

Yang, X. Z., H. Keppler, C. McCammon, and H. W. Ni (2012), Electrical conductivity of orthopyroxene and plagioclase in the lower crust, *Contrib. Mineral. Petrol.*, *163*, 33–48, doi:10.1007/s00410-011-0657-9.

Yoshino, T., and F. Noritake (2011), Unstable graphite films on grain boundaries in crustal rocks, *Earth Plane*, *Sci. Lett.*, *306*, 186–192.

Yoshino, T., T. Matsuzaki, S. Yamashita, and T. Katsura (2006), Hydrous olivine unable to account for conductivity anomaly at the top of the asthenosphere, *Nature*, *443*, 973–976, doi:10.1038/nature05223.

Yoshino, T., T. Matsuzaki, A. Shatskiy, and T. Katsura (2009), The effect of water on the electrical conductivity of olivine aggregates and its implications for the electrical structure of the upper mantle, *Earth Planet*, *Sci. Lett.*, *288*, 291–300, doi:10.1016/j.epsl.2009.09.032.

Zaidi, H., F. Robert, and D. Paulmier (1995), Influence of adsorbed gases on the surface energy of graphite: Consequence on the friction behavior, *Thin Solid Films*, *264*, 46–51.